

## Experimental acute myocardial infarction: telocytes involvement in neo-angiogenesis

C. G. Manole<sup>a, b</sup>, V. Cismaşiu<sup>b</sup>, Mihaela Gherghiceanu<sup>b</sup>, L. M. Popescu<sup>a, b, c, \*</sup>

<sup>a</sup> Department of Cellular and Molecular Medicine, 'Carol Davila' University of Medicine and Pharmacy, Bucharest, Romania

<sup>b</sup> Division of Advanced Studies, 'Victor Babeş' National Institute of Pathology, Bucharest, Romania

<sup>c</sup> National Academy of Sciences, Bucharest, Romania

Received: April 20, 2011; Accepted: August 25, 2011

### Abstract

We used rat experimental myocardial infarction to study the ultrastructural recovery, especially neo-angiogenesis in the infarction border zone. We were interested in the possible role(s) of telocytes (TCs), a novel type of interstitial cell very recently discovered in myocardium (see [www.telocytes.com](http://www.telocytes.com)). Electron microscopy, immunocytochemistry and analysis of several proangiogenic microRNAs provided evidence for TC involvement in neo-angiogenesis after myocardial infarction. Electron microscopy showed the close spatial association of TCs with neoangiogenetic elements. Higher resolution images provided the following information: (a) the intercellular space between the abluminal face of endothelium and its surrounding TCs is frequently less than 50 nm; (b) TCs establish multiple direct nanocontacts with endothelial cells, where the extracellular space seems obliterated; such nanocontacts have a length of 0.4–1.5 µm; (c) the absence of basal membrane on the abluminal face of endothelial cell. Besides the physical contacts (either nanoscopic or microscopic) TCs presumably contribute to neo-angiogenesis *via* paracrine secretion (as shown by immunocytochemistry for VEGF or NOS2). Last but not least, TCs contain measurable quantities of angiogenic microRNAs (*e.g.* let-7e, 10a, 21, 27b, 100, 126-3p, 130a, 143, 155, 503). Taken together, the direct (physical) contact of TCs with endothelial tubes, as well as the indirect (chemical) positive influence within the 'angiogenic zones', suggests an important participation of TCs in neo-angiogenesis during the late stage of myocardial infarction.

**Keywords:** acute myocardial infarction • neo-angiogenesis • telocytes • endothelial cells • microRNAs • angiogenic zones • VEGF • NO synthase 2 • cardiomyocytes

### Introduction

Understanding the mechanisms of cardiac regeneration and repair after myocardial infarction is an important subject of contemporary medicine. The effects of experimental myocardial infarction were frequently reported [1–16]. Indeed, according to PubMed database, there are 3840 titles (from 1956 to August 2011) for the 'rat myocardium infarction' search! Experimental myocardial infarction shows two different zones: (a) the central zone where most of the normal myocardial components (cardiomyocytes – CMs, interstitial cells, capillaries) are disintegrated; (b) the border zone with acute hypertrophy, followed by chronic hypertrophy (even after the healing process is over), and tissue remodelling.

Previously, our group documented the presence of a distinct interstitial cell type in heart [17–19]. The term telocyte (TC) was coined for these cells, and telopodes (Tps) for their very long (tens to hundreds of µm) and moniliform prolongations [20–23]. Tps are an alternation of thin segments (podomers) and dilated segments (podoms). Podomers are very thin (up to 0.2 µm), below the resolving power of light microscopy, explaining the fact that TCs were overlooked [20–23]. The concept of TC was taken up by other Laboratories [24–36]. Moreover, Liu *et al.* [37] reported the distribution of TCs in rat heart: more in atria than in ventricles (20 *versus* 9 cells/mm<sup>2</sup>) and significantly higher in subepicardium than in endocardium (18 *versus* 7 cells/mm<sup>2</sup>).

The aim of this study was to assess the involvement of TCs in the neo-vascularization process in the border zone of infarction. By electron microscopy and immunocytochemistry we observed TCs in the border zone 30 days after myocardial infarction. TCs appear in close spatial relationships with blood vessels and immunopositive

\*Correspondence to: L.M. POPESCU, M.D., Ph.D.,  
Department of Cellular and Molecular Medicine,  
'Carol Davila' University of Medicine and Pharmacy,  
P.O. Box 35-29, Bucharest 35, Romania.  
E-mail: LMP@jcmm.org

for VEGF and NOS2. By microRNA qPCR we found, at the level of TC body, the expression of various angiogenic microRNAs. Therefore, TCs appear as key-players in neo-angiogenesis within the 'angiogenic zones' of the border zone infarction.

## Materials and methods

### Rat surgery

A number of four Wistar male rats (average weight of 270 g) have undergone surgery for ligation of left anterior descending coronary artery (LADC), in accordance with the Institutional Ethical Committee approval. For rat myocardial infarction the experimental protocol was adapted from that used by Odörfer *et al.* [38].

One day before surgery, each animal received injectable antibiotic enrofloxacin (Baytril; Bayer, Leverkusen, Germany) and pretreated metamizol sodium (Algocalmin; Zentiva, Bucharest, Romania). Anaesthesia was made with a cocktail consisting of acepromazine maleate (Neurotranq; Alfasan, Woerden, Holland) and Ketamine hydrochloride (Ketamine HCL<sup>®</sup>; Kepro, Deventer, Holland). Animals were intubated using a Teflon catheter (16G/φ 1.7; Suru International Pvt. Ltd., Mumbai, India). Each animal was positioned on the right side on a 38°C heat-held plate (Harvard Apparatus, Holliston, MA, USA). During the surgery each animal was connected to a ventilator CWE SAR-830/P ventilator (Ardmore, PA, USA) with external air pump (ASF Inc, Norcross, GA, USA), set at a rate of 52 breaths per minute with a volume of 8 ml of air. After the surgical tolerance was examined and no more control reflexes were triggered, the thorax was opened between the third and fourth ribs, by blunt splitting of the Mm. intercostales. Pericardium was opened and arteria coronaria sinistra was proximally surrounded Vicryl 5-0 (SMI, Hünningen, Belgium) with a surgical knot. In all cases the ligation was made immediately below the lower margin of the left auricle. The acute occlusion of LADC of the ligature was verified by the pallor of the unsupplied myocardium. The closure of the chest was performed using 3–4 stitches Vicryl 4-0 (SMI, Hünningen, Belgium) between cranial and caudal ribs. The lung was previously expanded to prevent pneumothorax. Each muscular layer was continuously sutured with Vicryl 4-0 (SMI, Hünningen, Belgium). The surgical wound was bacteriostatic covered with oxytetracycline (Oxyvet, Veterin, Attiki, Greece). After the surgery, the animal was disconnected from the ventilator and extubated. Once the reflexes appeared, the animal was moved in a cage with sterile wood chips. Subsequently, the animal received metamizole sodium (Algocalmin; Zentiva, Bucharest, Romania) for immediate analgesia. The aftercare medication was for 3 days after the surgery, contained enrofloxacin, for antibiotic therapy and sodium metamizole for pain therapy.

The LV dysfunction in this experimental model of rat myocardial infarction was assessed by echocardiography, using a Vevo 770 Imaging System (Visualsonics, Toronto, Canada) with a 15–22.5 KHz transducer.

### Transmission electron microscopy

Thirty days after permanent ligation of the LADC, the rats were killed by cervical dislocation. The hearts were harvested. Small fragments (1 mm<sup>3</sup>) of rat ventricular myocardium (infarction area and border zone) were processed for transmission electron microscopy (TEM) according to routine Epon-embedding procedure, previously described [17, 19, 39–41].

The thin and thick sections were cut with a diamond knife using an RMC ultramicrotome (Boeckeler Instruments, Inc., Tucson, AZ, USA) and double-stained with 1% uranyl acetate and Reynolds lead citrate. Sections of about 60-nm-thin were examined with a Morgagni 286 transmission electron microscope (FEI Company, Eindhoven, The Netherlands) at 60 kV. Digital electron micrographs were recorded with a MegaView III CCD using ITEM-SIS software (Olympus, Soft Imaging System GmbH, Monster, Germany). On TEM images TCs, Tps, blood vessels were digitally coloured in blue and brown using Adobe<sup>®</sup> Photoshop CS3 to mark them out.

### Immunocytochemistry

Immunohistochemistry for VEGF and NOS2 was done according to the protocol reported by Suciú *et al.* [42] and Popescu *et al.* [43].

### Laser capture microdissection (LCM), RNA isolation and microRNA qPCR

Cell cultures and methods used were previously described [44]. Cells were fixed with absolute ethanol and stained with Giemsa. LCM was performed using the PALM MicroBeam system (Carl Zeiss MicroImaging GmbH, Jena, Germany) in accordance with the manufacturer protocols. For each sample, TC and control, a total of 500 cells were harvested in two separate experiments. The catapulted cells were captured and lysed in Epp tube caps filled with 30 ml of TRI Reagent (Sigma-Aldrich, St. Louis, MO, USA). Total RNA was extracted using the standard protocol recommended by the manufacturer (Sigma-Aldrich). The purity of RNA was evaluated with the NanoDrop ND-1000 Spectrophotometer (Thermo Scientific, Waltham, MA, USA). For cDNA synthesis we used QuantiMir RT (System Biosciences, San Francisco, CA, USA) according to manufacturer instructions. The cDNA templates were then quantified in a real-time SYBR Green qPCR reaction (iCycler system and software, Bio-Rad, Hercules, CA, USA) using universal reverse primers and microRNA-specific forward primers (System Biosciences, San Francisco, CA, USA). Mouse U6 snRNA and RNU43 were used as endogenous controls. The negative control was performed by omitting the reverse transcriptase.

### Statistics

The data are represented as mean + S.D. of three experiments and two-tailed *P* values of less than 0.05 were considered as statistically significant.

## Results

In all the cases the central zone and the corresponding border zone of infarction were clearly distinguishable. The lesion development corresponded to that previously described in literature. Figures 1–4 show TEM modifications of the border zone at specific intervals after LADC ligation: 1 day, 2 days, 1 week and 1 month.

Figure 1 shows an area of border zone of myocardial infarction, 1 day after the ligation of LADC. The general aspect is typical for an acute *inflammatory reaction*. The dominant population is

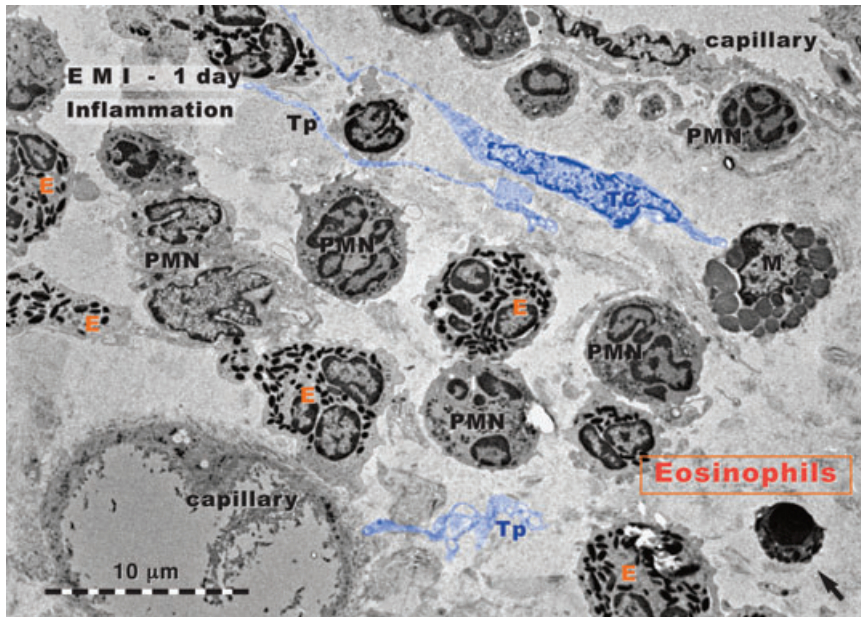


**Fig. 1** Rat experimental myocardial infarction. Border zone: 1-day-old. Transmission electron microscopy. The inflammatory granulocyte reaction dominates: granulocyte infiltration, mainly eosinophils (E) and neutrophils (PMN); a mast cell (M) is visible; the arrow indicates an apoptotic cell. A telocyte (TC) and several telopodes (Tp) are digitally blue coloured.

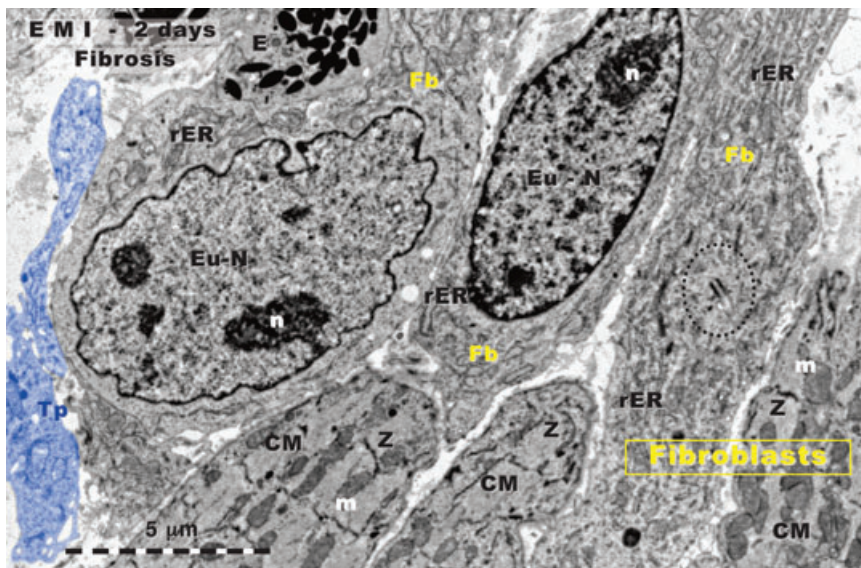


**Fig. 2** Rat experimental myocardial infarction. Border zone: 2-day-old. Transmission electron microscopy. Three fibroblasts (upper part) intermingle with three cardiomyocytes (lower part). The accumulation of fibroblasts indicates the beginning of fibrosis. Note that usually, in normal myocardium, there are no fibroblast clusters; Fb: fibroblast; rER: rough endoplasmic reticulum; Eu-N: euchromatin; n: nucleolus; CM: cardiomyocyte; m: mitochondria; Z: Z line. Centriole presence (black dotted line) suggests fibroblast mitosis. Tp: telopode (digitally blue coloured); E: eosinophil.

represented by granulocytes: eosinophils and polymorphonuclear neutrophils. The lumen of capillaries is dilated, presumably due to the hypoxic conditions at the level of the border zone. Apparently, TCs are not so frequently found like in normal myocardium. However, we did not make a quantitative comparison.

Figure 2 shows a TEM aspect from the border zone, 2 days after the ligation of LADC. The most visible modification is *fibroblast proliferation*. Incidentally, Figure 2 presents three typical fibroblasts and three CMs. However, in normal myocardium the ratio fibroblasts:CMs is not 1:1 (!). Noteworthy, a previous study of our Laboratory [45] reported a morphometric results, by stere-

ology, which indicated that CMs in rat ventricular myocardium occupy 76% and fibroblasts only 1.5% of myocardial volume (the remaining percentage corresponds to extracellular matrix, endothelial cells, TC and other interstitial cells). Thus, in our opinion, after 2 days of myocardial infarction the dominant phenomenon is the beginning of *fibrosis*, which is primarily produced by fibroblast proliferation. Again, TCs presence seems to be not so frequent like in normal myocardium, but no direct quantitative comparison was made.

Figure 3 demonstrates the presence of *myofibroblasts* (cells which share features with Fb and with smooth muscle cells [46])



**Fig. 3** Rat experimental myocardial infarction. Border zone: 7-day-old. Transmission electron microscopy. Note the presence of a typical myofibroblast. Such cells are responsible for matrix remodelling. Myofibroblasts have intermediate features between fibroblasts and smooth muscle cells: prominent rough endoplasmic reticulum (rER, like fibroblasts), and myofilaments (mf, like smooth muscle cells) located under the cell membrane. The characteristic ultrastructural feature, the fibronexus, which is a cell-to-stroma attachment, is highlighted by black dotted circle. E: eosinophil; coll: collagen fibrils.

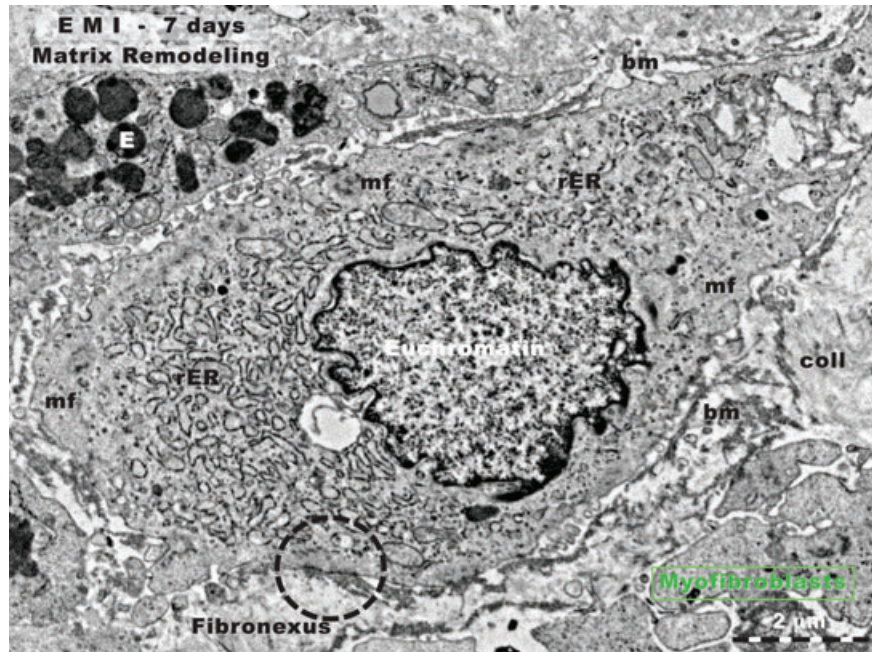
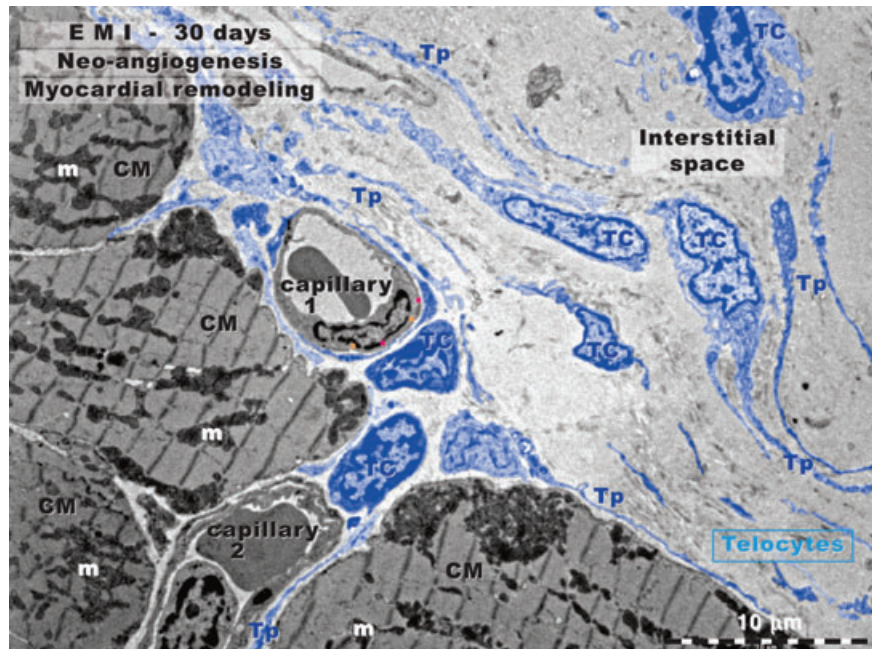


**Fig. 4** Rat experimental myocardial infarction. Border zone: 30-day-old. Transmission electron microscopy. This low magnification view shows four cardiomyocytes (CM), two blood capillaries (1 and 2) and numerous telocytes (TC) with long and slender telopodes (Tp). Note the close spatial relationship between TC/Tp and capillary-1 wall (endothelium). Capillary-1 is presumably a neo-capillary created in the interstitial space. Capillary-2, between three cardiomyocytes (CMs), has a TC and Tps in the vicinity, but the distance between abluminal membrane of endothelium and TC/Tp plasma membrane is wider. Thus, capillary-2 is probably an 'old' capillary.



in the border zone, seven days after the acute occlusion of LADC. Abundant rER is obvious (like in active fibroblasts), as well as myofilaments and caveolae (like in smooth muscle cells). Moreover, this myofibroblast presents a very characteristic feature: a cell-to-matrix adhesive structure – fibronexus (Fig. 3) – which enables the positive diagnostic [47, 48]. The myofibroblasts are particularly responsible for *matrix remodelling*.

Thirty days after the LADC ligation, a process of recovering characterizes the border zone of the myocardial infarction (Fig. 4). CMs begin to have normal ultrastructural appearance. In the interstitium, the number of TCs is clearly increased in comparison with normal myocardium. TCs/Tps have close spatial relationships with blood capillaries. However, the distances separating the Tps and abluminal front of endothelial cells and Tps are different for capillary of neo-

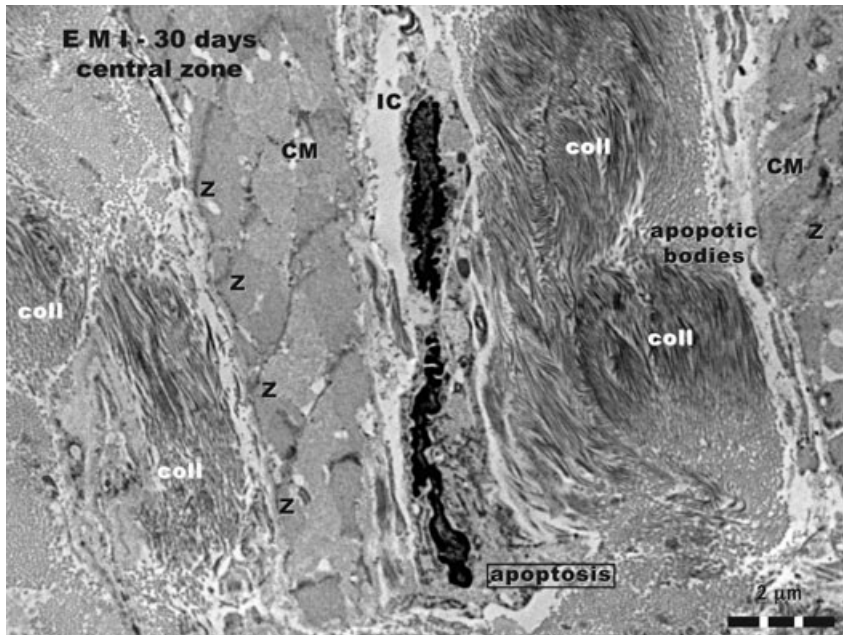


**Fig. 5** Rat experimental myocardial infarction. Central zone of the scar: 30-day-old; transmission electron microscopy. Three structural elements can be recognized in this image: (a) abundant deposits of collagen fibrils (coll), cross or obliquely cut; (b) damaged cardiomyocytes (CM), 'homogenized' myofibrils, only positions of Z lines being recognizable; (c) apoptotic interstitial cells (IC), and apoptotic bodies.

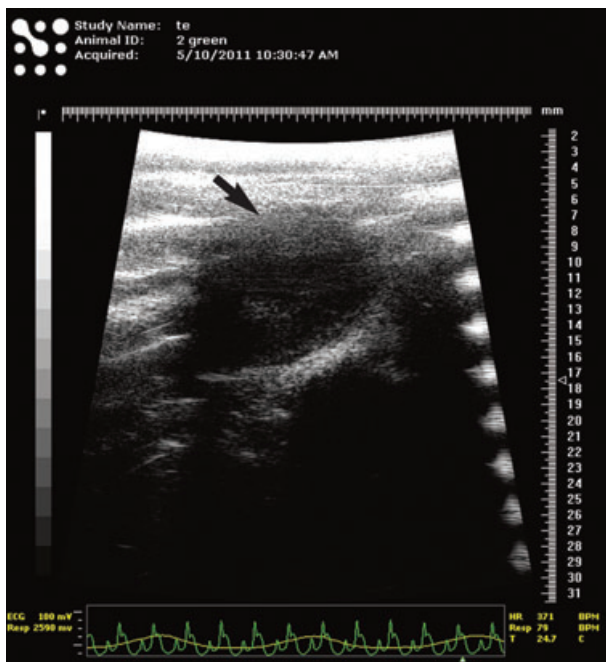


**Fig. 6** Typical echocardiogram of rat experimental myocardial infarction (30-day-old). The black arrow indicates the dyskinetic region of ventricular free wall corresponding to myocardial infarction area. The corresponding ECG in the lower part of the figure shows typical elevation of ST segment, suggestive for acute myocardial infarction.

formation (e.g. capillary-1 in Fig. 4) versus preexisting capillaries (e.g. capillary-2 in Fig. 4). Digitally measurements of the nanoscopic and microscopic distances resulted in the following results:

- (a) **Capillary of neo-formation:** there are two situations:
  - i. Either the extracellular space between abluminal endothelial cell membrane and the Tp membrane is obliterated, both membranes coming in direct physical contact (less than 10 nm);
  - ii. A very narrow intercellular cleft (comparable with canonical synaptic cleft !) with dimensions ranging between:
    - a minimum of about 80 nm (red dots in Fig. 4), and
    - a maximum of about 120 nm (orange dots in Fig. 4).
- (b) **Preexisting capillaries:** the widths of spaces separating the two plasma membranes (endothelial and telopodic) are wider, being around 200 nm (below the practical resolving power of light microscopy).

Figure 5 shows ultrastructural modifications in the *central zone*, after 30 days of myocardial infarction (compare with the 'border zone' of Figs 1–4). Abundant deposits of collagen are visible. CMs have discontinuous Z lines and myofibrils look 'homogenized'. Cells have some characteristics of *apoptosis*: shrinkage of the cells, condensation of chromatin, cellular fragmentation (observable at cellular poles, mainly). Apoptotic bodies can also be seen. The dyskinetic areas of infarction (like in Fig. 5) were documented by echocardiography and ECG. Figure 6 corresponds to the functional damage of the left ventriculum, as a result of LADC ligation.

Figures 7 and 8 provide additional evidence for the involvement of TCs in neo-angiogenesis after 30 days of myocardial infarction. The number of TCs and Tps is increased in the border zone. Their close spatial relationships with new-formed blood capillaries is obvious. In Figure 7, Tp1 surrounds and establishes multiple *nanocontacts* with the new-formed capillary. The length of these contacts ranges between 0.36 and 1.45  $\mu\text{m}$ , as it is shown at higher magnification in Figure 8. The width of the space between



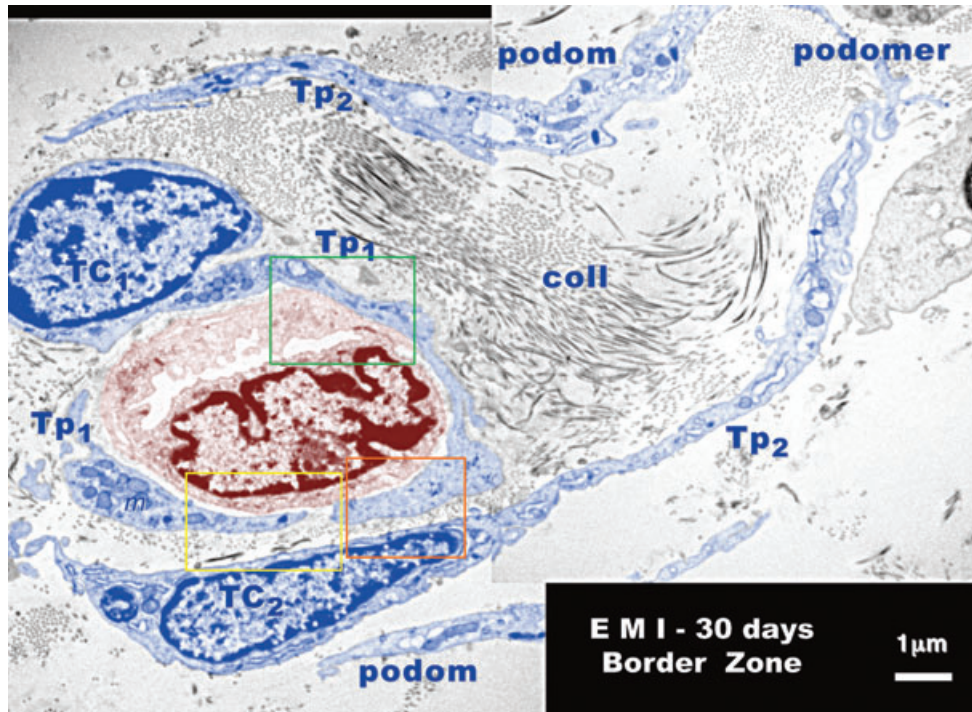


**Fig. 7** Rat experimental myocardial infarction. Border zone: 30-day-old. Transmission electron microscopy. A new-formed blood capillary with an anfractuous and narrow lumen is shown (brown colour) in the mass of collagen fibrils (coll) of the scar. This is surrounded by two telocytes (TC1 and TC2 - blue colour) and their corresponding telopodes (TP1 and TP2). Typically podoms (dilated portions) and the intercalary podomers (thin portions of Tp) can be observed. At the level of podoms there are many mitochondria (m), elements of endoplasmic reticulum and caveolae. Note the close spatial relationships between telopodes and endothelial cells. The space between telopodes and the membrane of endothelial cell is occasionally less than 50 nm and there is no visible endothelial basal lamina.

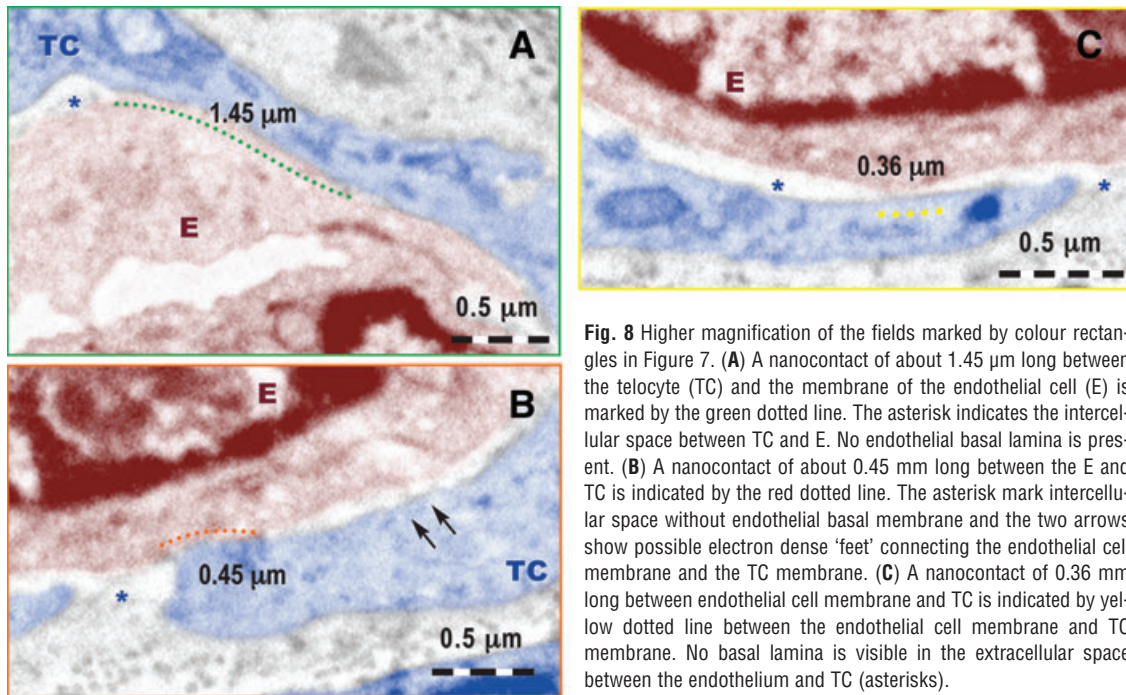


**Fig. 8** Higher magnification of the fields marked by colour rectangles in Figure 7. (A) A nanocontact of about 1.45 μm long between the telocyte (TC) and the membrane of the endothelial cell (E) is marked by the green dotted line. The asterisk indicates the intercellular space between TC and E. No endothelial basal lamina is present. (B) A nanocontact of about 0.45 μm long between the E and TC is indicated by the red dotted line. The asterisk mark intercellular space without endothelial basal membrane and the two arrows show possible electron dense 'feet' connecting the endothelial cell membrane and the TC membrane. (C) A nanocontact of 0.36 μm long between endothelial cell membrane and TC is indicated by yellow dotted line between the endothelial cell membrane and TC membrane. No basal lamina is visible in the extracellular space between the endothelium and TC (asterisks).

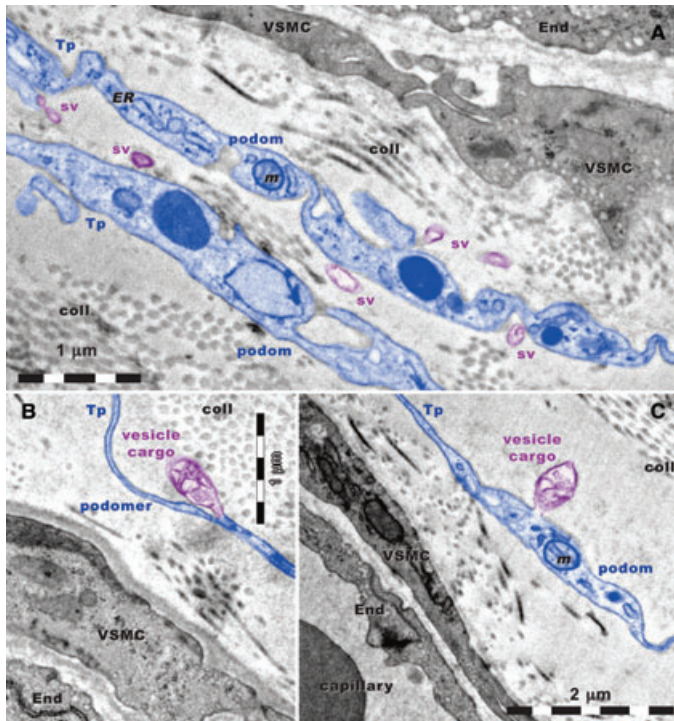


**Fig. 9** Rat experimental myocardial infarction. Border zone: 30-day-old. Transmission electron microscopy. Telopodes (Tp) are situated in close vicinity of blood vessels. Vascular smooth muscle cells (VSMC) and endothelial cells (End) have many caveolae. Note the alternation of podoms and podomers. Podoms contain: mitochondria (m), and endoplasmic reticulum (ER) and caveolae (cav). (A) Shed vesicles (sv) are released from podoms. A vesicle cargo multivesicular is formed from a podomer (B) and another one is formed from a podom (C). coll: collagen.

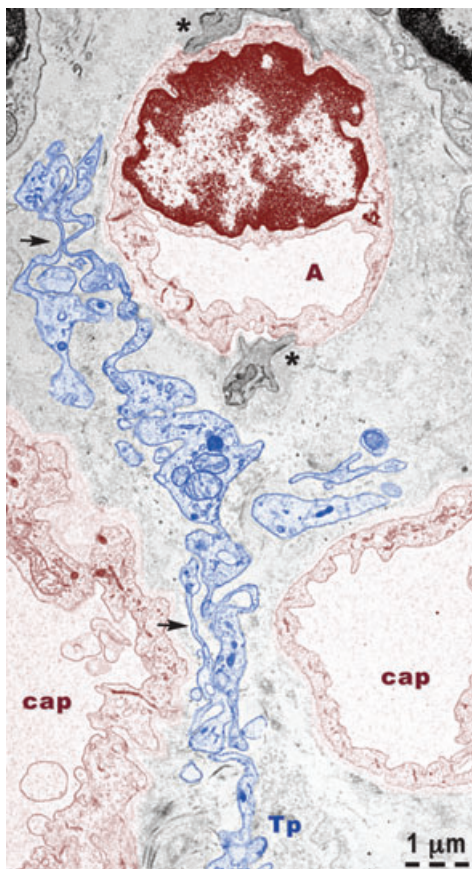


**Fig. 10** Rat experimental myocardial infarction. Border zone: 30-day-old. Transmission electron microscopy. A telopode (Tp - blue colour) is located between three new-formed capillaries (cap). At the level of capillary A, basal lamina and fragments of pericytes (asterisks) are visible. The capillary endothelium (brown colour) has many vesicles of transcytosis. Note the alternation of podoms (containing mitochondria, endoplasmic reticulum and caveolae) and podomers (thin segments) - arrows.

the plasma membrane of the Tp and the endothelial cell membrane is 50–70 nm (Fig. 8B) or 40–100 nm (Fig. 8C). Within the extracellular space some electron-dense 'feet', with a 'height' of about 60 nm, seem connect endothelial and TC cell membranes. *The endothelial basal lamina is absent along these nanocontacts.*

In the vicinity of new-formed blood capillaries, TCs and Tps release shed vesicles and vesicle groups from podoms and/or podomers (Fig. 9). In Figure 9A, the visible shed vesicles have a diameter between 60 and 330 nm. The vesicle groups in Figure 9B and C are of 730/280 nm and 710/470 nm, respectively. They have a heterogeneous content and seem to be involved in heterocellular communication.

For underlining the involvement of TC in angiogenesis, Figures 9 and 10 show the strategic positions of the Tps either among new-formed blood vessels (Fig. 9), or surrounding them (Fig. 10). The *new-formed blood vessels* have typical tall endothelial cells with numerous organelles and a narrow and anfractuous lumen (Figs 11 and 12). The endothelium has many transcytosis vesicles.

*Immunocytochemistry* performed show positive reactions of TC for VEGF and NOS2 in normal heart (Fig. 13). In the border zone of the myocardial infarction positive expression for both VEGF and NOS2 is shown by cells with similar appearance with



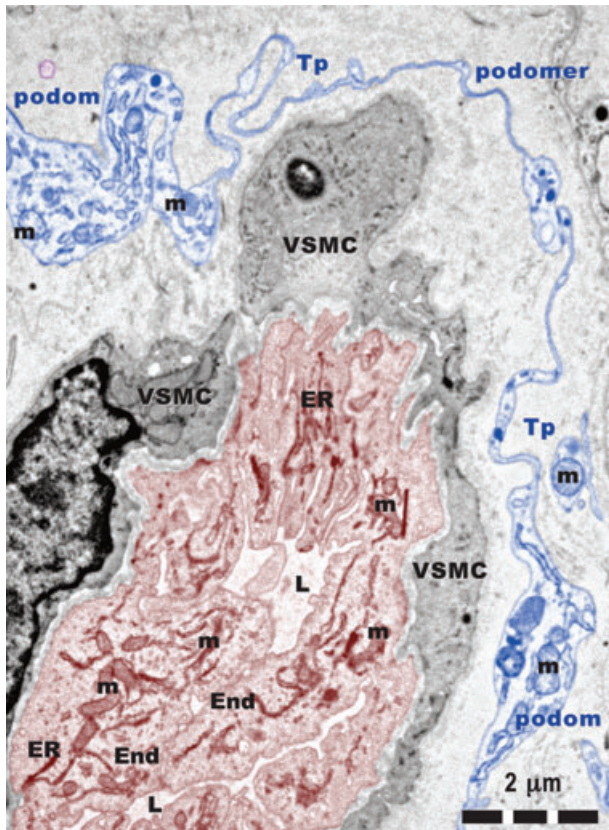


**Fig. 11** Rat experimental myocardial infarction. Border zone: 30-day-old. Arteriogenesis. Transmission electron microscopy. A telopode (Tp) surrounding a new-formed blood vessel. Tall endothelial cells (End) with numerous mitochondria (m) and endoplasmic reticulum (ER) cisternae, circumvent a narrow and irregular lumen (L). VSMC: vascular smooth muscle cell.

TC. These cells are located in the close vicinity of blood vessels having close spatial relationships with them.

Because the data suggest that TCs are intimately connected with the neovascularization after myocardial infarction, we have investigated whether TCs are expressing angiogenic microRNAs. Cardiac TCs were isolated from the first-passage cultures by laser capture microdissection (Fig. 14) and the expressions of microRNAs were determined by RT-qPCR as previously described [41]. The data presented in Figure 15 show that several microRNAs with angiogenic functions are present in TCs.

## Discussion

Angiogenesis is essential for myocardium repair and remodelling after myocardium infarction. Direct intercellular communication of endothelial cells with other cells is crucial for an efficient vascular formation [49]. The direct contact of endothelial progenitors with

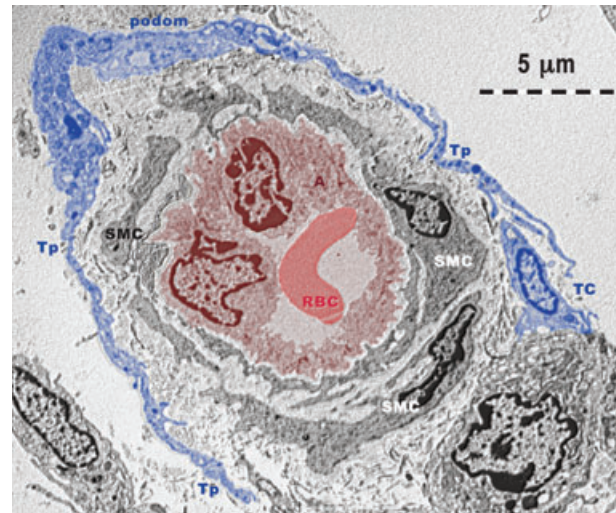


**Fig. 12** Rat experimental myocardial infarction. Border zone: 30-day-old. Arteriogenesis. Transmission electron microscopy. Telopodes (Tp) with typical podoms and podomers, from at least one telocyte (TC - blue colour) are encircling an arteriole (A: brown colour). Note: (a) the endothelium (brown coloured) surrounding the lumen which contains a red blood cell (RBC: red colour); (b) lamina elastica interna – a clear space surrounding the endothelium; (c) 2–3 layers of smooth muscle cells (SMC).

‘ventricle slices’ (presumably TC !?) seems of importance for angiogenesis [50].

It is widely accepted that after 30 days of experimental myocardial infarction, the border zone of the lesion is characterized by neo-angiogenesis [13, 51]. Generally, there are many types of angiogenic factors: *e.g.* (a) growth factors and their receptors; (b) matrix proteins and proteases; (c) adhesion molecules; (d) microRNAs and transcription factors.

We used a trio of methods (morphology – transmission electron microscopy; immunocytochemistry – VEGF and NOS2 expression and molecular biology – angiogenic microRNAs expression), which showed the involvement of TC in neo-angiogenesis, in the border zone.

## Electron microscopy

In the border zone of myocardial infarction the relationships between TCs and new-formed blood vessels are obvious. TCs have close vicinity with new-formed blood vessels (capillary and/or arterioles), but also with the preexisting blood vessels. The space between TCs/Tps and the abluminal face of the endothelium is sometimes less than 50 nm, and therefore in the macromolecular-interaction range. Anyway, TCs establish heterocellular contacts also with CM as it was previously described [52].

TCs/Tps release shed vesicles or exosomes. The roles of exosomes are not understood, but they seem to play an important role in intercellular communication [53]. Shed vesicles



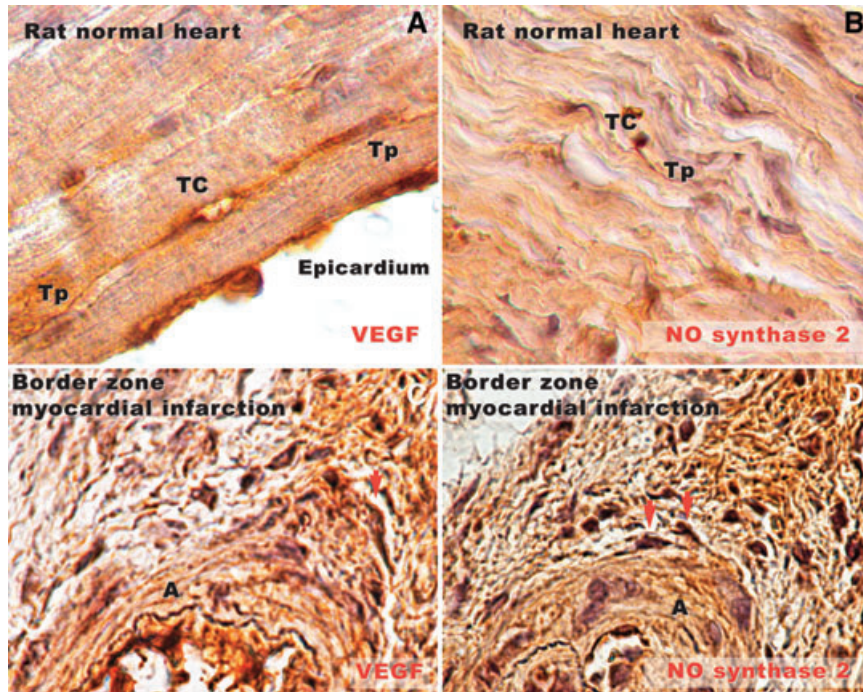


**Fig. 13** Rat normal heart tissue (**A, B**) and border zone of infarcted heart tissue (**C, D**) in experimental myocardial infarction (30-day-old). (**A**) Immunostaining for VEGF demonstrates positive expression in the subepicardial area. A silhouette of a telocyte (TC) can be seen parallel with the epicardium. Very long and slender telopodes (Tp) are obvious. (**B**) Positive expression for NOS2 in rat normal myocardium. A Tp splits dichotomously near the TC cell body, and runs parallel with cardiac fibres. (**C**) In the border zone of infarcted heart tissue, near a new-formed arteriole (**A**), a cell (most probably a TC, taking into account the morphology) is positive for VEGF (arrow). (**D**) Positive reaction for NOS2 in two different cells (arrows) near a new-formed blood vessel in the border zone of infarction. Their prolongations are neighbouring the blood vessel wall. Original magnifications: (**A, B**) – 100 $\times$ ; (**C, D**) – 60 $\times$ .

and exosomes presumably transfer macromolecules (*e.g.* microRNAs, proteins), which cannot be released through the intact plasmalema. Our results suggest some possible mechanisms for TCs involvement in ‘angiogenic zones’: either direct (physical contact), or indirect (chemical signalling) (Fig. 16). An ‘exosome therapy’ could be taken into account as a future possibility [54, 55].

## Immunocytochemistry

Immunocytochemistry done for NO and VEGF confirmed our previous studies regarding the presence of TC in normal myocardium. After 30 days of myocardial infarction, interstitial cells similar to those described in normal heart are found in affected myocardium. At the level of cell body and cell prolongations these cells have positive expression for NO and VEGF, as it was previously reported in other organs [41–43]. These data could be relevant because TC may promote and/or modulate angiogenesis after myocardial infarction *via* VEGF and/or NO secretion.

## Angiogenic microRNAs

The human genome encodes 1048 microRNAs, which virtually regulate all biological processes [56]. In addition, microRNAs are predicted to regulate the expression of more than one-third of human protein-coding genes. There is increasing evidence that miRNAs

play important roles in vascular development as well as in vascular diseases. Here we show that several pro-angiogenic microRNAs are expressed by TCs: *e.g.* miR 126 [57], miR130a [58], let-7 family [59, 60], miR-10 [61], miR-155 [62], miR-503 [63]. Another pro-angiogenic factor, miR-21, induces HIF-1 $\alpha$  and VEGF expression and activates both AKT and ERK pathways for mediating angiogenesis [64]. The clusters of miRNAs which include miR-27 are highly expressed in ECs and repress the anti-angiogenic proteins Sprouty2 and Sema6A [65]. The proliferation, migration and tube formation of ECs are regulated also by miR-100 [66]. Also, miR-143 is abundant microRNA in vascular smooth muscle cells and it was found down-regulated in diseased arteries [67].

Interestingly, TCs express both stromal specific [44] and vascular smooth muscle specific (miR-143/145) microRNAs as well as pro-angiogenic miRs highly enriched in endothelial cells (such as miR-126). Such expression patterns may support the view that several cell type specific signalling pathways converge in TCs and further suggests a complex regulatory mechanism driven by telocytes during the cardiac regeneration. In addition, TCs may secrete microvesicles or exosomes containing specific cocktail(s) of miRNAs, which are internalized by surrounding cells (such as endothelial and smooth muscle cells). Thus, these cells can modulate the angiogenesis process through paracrine signals.

Figure 16 presents the essential data of our results and proposals for the mechanisms involved in neo-angiogenesis in the border zone of myocardial infarction, including the microRNA participation *via* secretion (transport by shed vesicles and/or exosomes), that we call ‘microcrine’ phenomenon. The possible

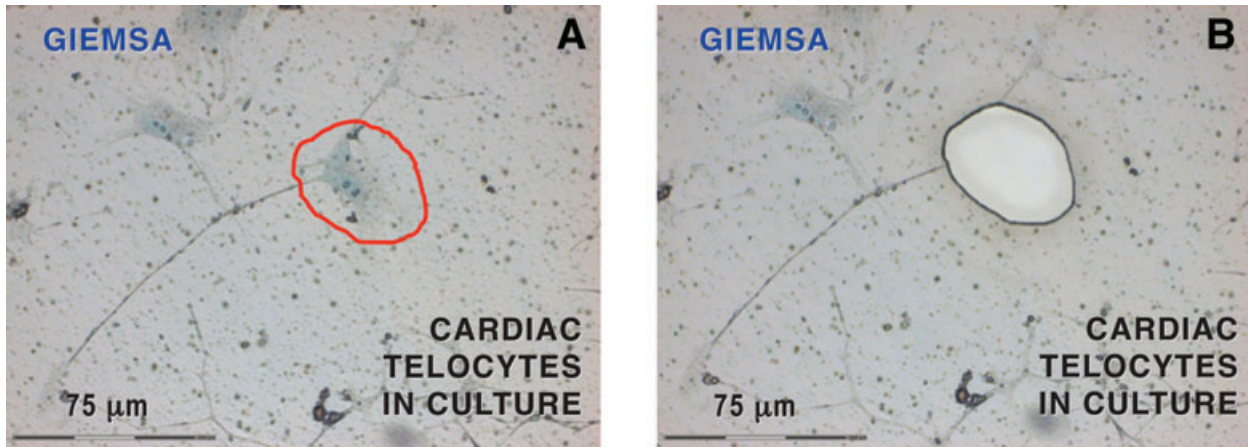


**Fig. 14** Laser capture microdissection of cardiac telocytes in culture. Because other interstitial cells than telocytes might be present, only cells with 'multipolar' body and at least one prolongation of more than 50 mm long were considered telocytes. Such prolongations had typical telopode conformation, with podoms (dilated portions) and podomers (thin segments). (A) The telocyte body encircled by the red line was dissected out by laser capture microscopy. (B) The corresponding area of Figure 11A after microdissection. A total of 500 telocyte bodies were collected and analysed for microRNAs. 20× objective.

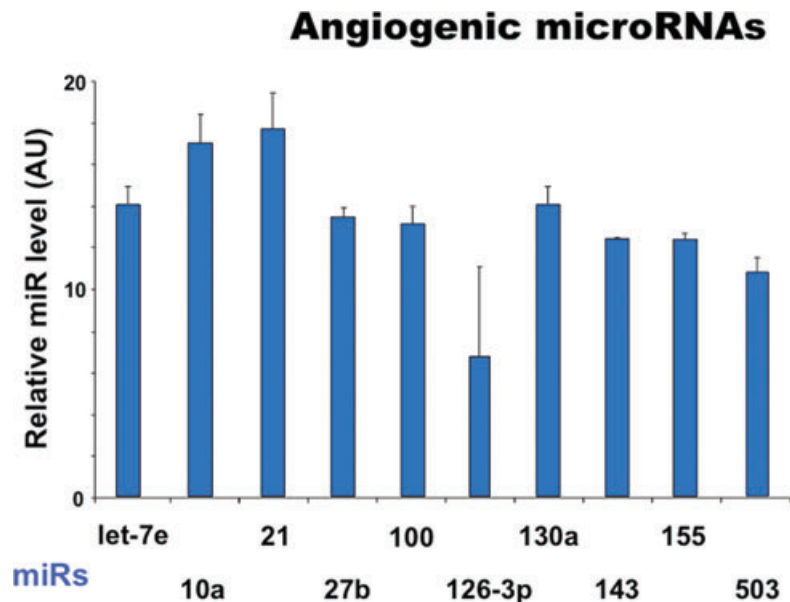


**Fig. 15** Expression levels of microRNAs up-regulated in telocytes. The relative expression was determined by real-time PCR. RNU43 snoRNA and U6 snRNA were used as normalizing controls. The error bars are mean + S.D. (n = 3) and the data are representative for two replicate experiments. AU: arbitrary units.

role(s) of TC in the maturation of capillaries into arteriolar vessels remains to be established.

There is a good correlation between electron microscopy and immunocytochemistry because it is well known that experimentally induced ischaemia results in a dramatic increase of VEGF levels in myocardium [68, 69]. Moreover, VEGF appears to act by local up-regulation of NO production [70, 71].

Since telocytes are CD34 positive [20, 23, 41, 43], our results support the assumption of Kumar & Caplice [72] that paracrine factors secreted by CD34 positive cells contribute significantly to angiogenesis. Moreover, very recently Sahoo *et al.* [73]

demonstrated that CD34 positive cells secrete vesicles (exosomes) that have independent angiogenic activity, both *in vitro* and *in vivo*. But Figure 9 (A-C) shows directly by electron microscopy that TCs release shed vesicles and group of such vesicles (as multivesicular bodies) in angiogenic areas of the myocardial infarction border zone. This may not be a simple coincidence.

Further studies are required to clarify the relationships between TCs and pericytes, because pericytes are cells involved in angiogenesis, too [74, 75]. Anyway, preliminary studies in our Laboratory showed that TC are PDGF-R positive, like pericytes, in other words PDGF-R is not a marker for pericytes (Popescu *et al.*, in preparation).



**Possible mechanisms of telocyte involvement in neo-angiogenesis  
in the border zone of myocardial infarction**

<b>DIRECT PHYSICAL CONTACT (no basal membrane)</b>	Aposition ("synapse-like") (intercellular space obliterated)	linear (long distance)	length: 0.45-1.45 $\mu\text{m}$
		spot ("finger" - like protrusion) (short distance)	length: 0.36 $\mu\text{m}$
	Nano-contact	"feet" (electron dense)	height: 60 nm
<b>INDIRECT CHEMICAL SIGNALING (secretion)</b>	Paracrine	NO ↑ ↓ VEGF	Through membrane With membrane:
	Microcrine	microRNAs	Shed vesicles: 60-330 nm & Exosomes:

Fig. 16 Possible mechanisms of telocyte involvement in neo-angiogenesis in the border zone of myocardial infarction.

Finally, we support the idea of Laflamme and Murry [36] that 'after more than a decade of furious activity' stem cells ... and neo-angiogenesis ... 'seem to be catching up with its promise'. A TC-based therapeutic neo-angiogenesis in myocardial infarction could have a significant clinical potential.

Debrecen, Hungary) for their constant help in realizing the echocardiography for operated rats. This paper is partially supported by the Sectorial Operational Programme Human Resources Development (SOPHRD), financed from the European Social Fund and by the Romanian Government under the contract number POSDRU/89/1.5/S/64153 (V.B.C.). Prof. L.M. Popescu thanks Cord Blood Center (Cluj) for financial assistance.

## Acknowledgements

The authors thank Professor Árpád Tósaki and Dr. Juhász Béla (Department of Pharmacology and Pharmacodynamics, University of

## Conflict of interest

The authors declare no conflicts of interest.

## References

- Caulfield J, Klionsky B. Myocardial ischemia and early infarction: an electron microscopic study. *Am J Pathol.* 1959; 35: 489–523.
- Page E, Polimeni PI. Ultrastructural changes in the ischemic zone bordering experimental infarcts in rat left ventricles. *Am J Pathol.* 1977; 87: 81–104.
- Gottlieb GJ, Kubo SH, Alonso DR. Ultrastructural characterization of the border zone surrounding early experimental myocardial infarcts in dogs. *Am J Pathol.* 1981; 103: 292–303.
- Axford-Gatley RA, Wilson GJ. The "border zone" in myocardial infarction. An ultrastructural study in the dog using an electron-dense blood flow marker. *Am J Pathol.* 1988; 131: 452–64.
- Schaper J. Ultrastructural changes of the myocardium in regional ischaemia and infarction. *Eur Heart J.* 1986; 7B: 3–9.
- Vracko R, Thorning D. Contractile cells in rat myocardial scar tissue. *Lab Invest.* 1991; 65: 214–27.
- Matsushita T, Oyamada M, Fujimoto K, et al. Remodeling of cell-cell and cell-extracellular matrix interactions at the border zone of rat myocardial infarcts. *Circ Res.* 1999; 85: 1046–55.
- Frangogiannis NG, Smith CW, Entman ML. The inflammatory response in myocardial infarction. *Cardiovasc Res.* 2002; 53: 31–47.
- Wang B, Ansari R, Sun Y, et al. The scar neovasculature after myocardial infarction in rats. *Am J Physiol Heart Circ Physiol.* 2005; 289: H108–13.
- Weber KT, Sun Y, Díez J. Fibrosis: a living tissue and the infarcted heart. *J Am Coll Cardiol.* 2008; 52: 2029–31.
- Zornoff LA, Paiva SA, Minicucci MF, et al. Experimental myocardium infarction in rats: analysis of the model. *Arq Bras Cardiol.* 2009; 93: 434–40, 426–32.
- Bharti S, Arora S, Arya DS. Evaluation of morphological changes in experimental models of myocardial infarction: electron and light microscopical evidence. In: A. Méndez-Vilas, J Díaz, editors.

- Microscopy: science, technology, applications and education. Formatex, Spain; 2010. p. 361–71.
13. **Jin P, Wang E, Wang YH, et al.** Central zone of myocardial infarction: a neglected target area for heart cell therapy. *J Cell Mol Med.* 2011; doi: 10.1111/j.1582-4934.2011.01408.x.
  14. **Ye KY, Black LD 3rd.** Strategies for tissue engineering cardiac constructs to affect functional repair following myocardial infarction. *J Cardiovasc Transl Res.* 2011; doi: 10.1007/s12265-011-9303-1.
  15. **Wang H, Liu Z, Li D, et al.** Injectable biodegradable hydrogels for embryonic stem cell transplantation: improved cardiac remodeling and function of myocardial infarction. *J Cell Mol Med.* 2011; doi: 10.1111/j.1582-4934.2011.01409.x
  16. **Wu Y, Yin X, Wijaya C, et al.** Acute myocardial infarction in rats. *J Vis Exp.* 2011; 48: 2464; doi: 10.3791/2464.
  17. **Popescu LM, Manole CG, Gherghiceanu M, et al.** Telocytes in human epicardium. *J Cell Mol Med.* 2010; 14: 2085–93.
  18. **Gherghiceanu M, Popescu LM.** Cardiomyocyte precursors and telocytes in epicardial stem cell niche: electron microscope images. *J Cell Mol Med.* 2010; 14: 871–7.
  19. **Gherghiceanu M, Manole CG, Popescu LM.** Telocytes in endocardium: electron microscope evidence. *J Cell Mol Med.* 2010; 14: 2330–4.
  20. **Popescu LM, Fausone-Pellegrini MS.** Telocytes – a case of serendipity: the winding way from interstitial cells of Cajal (ICC), via interstitial Cajal-like cells (ICLC) to telocytes. *J Cell Mol Med.* 2010; 14: 729–40.
  21. **Popescu LM.** Telocytes – a novel type of interstitial cells. In: Braisant O, Wakamatsu H, Kang I, Allegaert K, Lenbury Y, Wacholtz A, editors. Recent researches in modern medicine -HISTEM'11. Cambridge: WSEAS Press; 2011. p. 424–32.
  22. **Popescu LM.** The tandem: telocytes – stem cells. *Int J Biol Biomed Eng.* 2011; 2: 83–92.
  23. **Fausone-Pellegrini MS, Popescu LM.** Telocytes. *BioMol Concepts.* 2011; doi: 10.1515/BMC.2011.039.
  24. **Gittenberger-de Groot AC, Winter EM, Poelmann RE.** Epicardium-derived cells (EPDCs) in development, cardiac disease and repair of ischemia. *J Cell Mol Med.* 2010; 14: 1056–60.
  25. **Rupp H, Rupp TP, Alter P, et al.** Intrapericardial procedures for cardiac regeneration by stem cells: need for minimal invasive access (AttachLifter) to the normal pericardial cavity. *Herz.* 2010; 35: 458–65.
  26. **Zhou J, Zhang Y, Wen X, et al.** Telocytes accompanying cardiomyocyte in primary culture: two- and three-dimensional culture environment. *J Cell Mol Med.* 2010; 14: 2641–5.
  27. **Li TS, Cheng K, Lee ST, et al.** Cardiospheres recapitulate a niche-like microenvironment rich in stemness and cell-matrix interactions, rationalizing their enhanced functional potency for myocardial repair. *Stem Cells.* 2010; 28: 2088–98.
  28. **Klump D, Horch RE, Kneser U, et al.** Engineering skeletal muscle tissue – new perspectives *in vitro* and *in vivo*. *J Cell Mol Med.* 2010; 14: 2622–9.
  29. **Kostin S.** Types of cardiomyocyte death and clinical outcomes in patients with heart failure. *J Am Coll Cardiol.* 2011; 57: 1532–4.
  30. **Limana F, Capogrossi MC, Germani A.** The epicardium in cardiac repair: from the stem cell view. *Pharmacol Ther.* 2011; 129: 82–96.
  31. **Gard JJ, Asirvatham SJ.** The “slow pathway” potential: fact or fiction? *Circ Arrhythm Electrophysiol.* 2011; 4: 125–7.
  32. **Russell JL, Goetsch SC, Gaiano NR, et al.** A dynamic notch injury response activates epicardium and contributes to fibrosis repair. *Circ Res.* 2011; 108: 51–9.
  33. **Rusu MC, Pop F, Hostiu S, et al.** Extrahepatic and intrahepatic human portal interstitial Cajal cells. *Anat Rec.* 2011; 294: 1382–92.
  34. **Xiao J, Liang D, Chen YH.** The genetics of atrial fibrillation: from the bench to the bedside. *Annu Rev Genomics Hum Genet.* 2011; doi: 10.1146/annurev-genom-082410-101515.
  35. **Horst Ibelgaufs.** Cytokines & Cells Online Pathfinder Encyclopedia. 2011; <http://www.copewithcytokines.org/cope.cgi?key=telocytes>.
  36. **Laflamme MA, Murry CE.** Heart regeneration. *Nature.* 2011; 473: 326–35.
  37. **Liu JJ, Shen XT, Zheng X, et al.** Distribution of telocytes in the rat heart. *J Clin Rehabil Tiss Eng Res.* 2011; 15: 3546–8.
  38. **Odörfer KI, Walter I, Kleiter M, et al.** Role of endogenous bone marrow cells in long-term repair mechanisms after myocardial infarction. *J Cell Mol Med.* 2008; 12: 2867–74.
  39. **Mandache E, Gherghiceanu M, Macarie C, et al.** Telocytes in human isolated atrial amyloidosis: ultrastructural remodelling. *J Cell Mol Med.* 2010; 14: 2739–47.
  40. **Hinescu ME, Gherghiceanu M, Suciu L, et al.** Telocytes in pleura: two- and three-dimensional imaging by transmission electron microscopy. *Cell Tissue Res.* 2011; 343: 389–97.
  41. **Popescu LM, Gherghiceanu M, Suciu LC, et al.** Telocytes and putative stem cells in the lungs: electron microscopy, electron tomography, and laser scanning microscopy. *Cell Tissue Res.* 2011; doi: 10.1007/s00441-011-1229-z.
  42. **Suciu L, Popescu LM, Gherghiceanu M, et al.** Telocytes in human term placenta: morphology and phenotype. *Cells Tissues Organs.* 2010; 192: 325–39.
  43. **Popescu LM, Manole E, Serboiu CS, et al.** Identification of telocytes in skeletal muscle interstitium: implication for muscle regeneration. *J Cell Mol Med.* 2011; 15: 1379–92.
  44. **Cismasiu VB, Radu E, Popescu LM.** miR-193 expression differentiates telocytes from other stromal cells. *J Cell Mol Med.* 2011; 15: 1071–4.
  45. **Popescu LM, Gherghiceanu M, Hinescu ME, et al.** Insights into the interstitium of ventricular myocardium: interstitial Cajal-like cells (ICLC). *J Cell Mol Med.* 2006; 10: 429–58.
  46. **Eyden B.** The myofibroblast: phenotypic characterization as a prerequisite to understanding its functions in translational medicine. *J Cell Mol Med.* 2008; 12: 22–37.
  47. **Schurich W, Seemayer TA, Gabbiani G.** The myofibroblast: a quarter century after its discovery. *Am J Surg Pathol.* 1998; 22: 141–7.
  48. **Eyden B.** The myofibroblast: an assessment of controversial issues and a definition useful in diagnosis and research. *Ultrastruct Pathol.* 2001; 25: 39–50.
  49. **Eming SA, Hubbell JA.** Extracellular matrix in angiogenesis: dynamic structures with translational potential. *Exp Dermatol.* 2011; 20: 605–13.
  50. **Lupu M, Khalil M, Iordache F, et al.** Direct contact of umbilical cord blood endothelial progenitors with living cardiac tissue is a requirement for vascular tube-like structures formation. *J Cell Mol Med.* 2011; 15: 1914–26.
  51. **Zhao T, Zhao W, Chen Y, et al.** Vascular endothelial growth factor (VEGF)-A: role on cardiac angiogenesis following myocardial infarction. *Microvasc Res.* 2010; 80: 188–94.
  52. **Gherghiceanu M, Popescu LM.** Heterocellular communication in the heart: electron tomography of telocyte-myocyte junctions. *J Cell Mol Med.* 2011; 15: 1005–11.



53. **Rana S, Zöller M.** Exosome target cell selection and the importance of exosomal tetraspanins: a hypothesis. *Biochem Soc Trans.* 2011; 39: 559–62.
54. **Martinez MC, Andriantsitohaina R.** Microparticles in angiogenesis: therapeutic potential. *Circ Res.* 2011; 109: 110–9.
55. **Record M, Subra C, Silvente-Poirot S, et al.** Exosomes as intercellular signalosomes and pharmacological effectors. *Biochem Pharmacol.* 2011; 81: 1171–82.
56. **Sen CK.** MicroRNAs as new maestro conducting the expanding symphony orchestra of regenerative and reparative medicine. *Physiol Genomics.* 2011; 43: 517–20.
57. **Wang S, Aurora AB, Johnson BA, et al.** The endothelial-specific microRNA miR-126 governs vascular integrity and angiogenesis. *Dev Cell.* 2008; 15: 261–71.
58. **Chen Y, Gorski DH.** Regulation of angiogenesis through a microRNA (miR-130a) that down-regulates antiangiogenic homeobox genes GAX and HOXA5. *Blood.* 2008; 111: 1217–26.
59. **Kuehbach A, Urbich C, Zeiher AM, et al.** Role of Dicer and Drosha for endothelial microRNA expression and angiogenesis. *Circ Res.* 2007; 101: 59–68.
60. **Otsuka M, Zheng M, Hayashi M, et al.** Impaired microRNA processing causes corpus luteum insufficiency and infertility in mice. *J Clin Invest.* 2008; 118: 1944–54.
61. **Shen X, Fang J, Lv X, et al.** Heparin impairs angiogenesis through inhibition of MicroRNA-10b. *J Biol Chem.* 2011; 286: 26616–27.
62. **Urbich C, Kuehbach A, Dimmeler S.** Role of microRNAs in vascular diseases, inflammation, and angiogenesis. *Cardiovasc Res.* 2008; 79: 581–8.
63. **Caporali A, Meloni M, Völlenkle C, et al.** Deregulation of microRNA-503 contributes to diabetes mellitus-induced impairment of endothelial function and reparative angiogenesis after limb ischemia. *Circulation.* 2011; 123: 282–91.
64. **Liu LZ, Li C, Chen Q, et al.** MiR-21 induced angiogenesis through AKT and ERK activation and HIF-1 $\alpha$  expression. *PLoS One.* 2011; 6: e19139.
65. **Zhou Q, Gallagher R, Ufret-Vincenty R, et al.** Regulation of angiogenesis and choroidal neovascularization by members of microRNA-23~27~24 clusters. *Proc Natl Acad Sci USA.* 2011; 108: 8287–92.
66. **Grundmann S, Hans FP, Kinniry S, et al.** MicroRNA-100 regulates neovascularization by suppression of mammalian target of rapamycin in endothelial and vascular smooth muscle cells. *Circulation.* 2011; 123: 999–1009.
67. **Elia L, Quintavalle M, Zhang J, et al.** The knockout of miR-143 and -145 alters smooth muscle cell maintenance and vascular homeostasis in mice: correlates with human disease. *Cell Death Diff.* 2009; 16: 1590–8.
68. **Ferrara N, Davis-Smyth T.** The biology of vascular endothelial growth factor. *Endocr Rev.* 1997; 18: 4–25.
69. **Neufeld G, Cohen T, Gengrinovitch S, et al.** Vascular endothelial growth factor (VEGF) and its receptors. *FASEB J.* 1999; 13: 9–22.
70. **Morbidelli L, Chang CH, Douglas JG, et al.** Nitric oxide mediates mitogenic effect of VEGF on coronary venular endothelium. *Am J Physiol.* 1996; 270: H411–5.
71. **Murohara T, Asahara T, Silver M, et al.** Nitric oxide synthase modulates angiogenesis in response to tissue ischemia. *J Clin Invest.* 1998; 101: 2567–78.
72. **Kumar AH, Caplice NM.** Clinical potential of adult vascular progenitor cells. *Arterioscler Thromb Vasc Biol.* 2010; 30: 1080–7.
73. **Sahoo S, Klychko E, Thorne T, et al.** Exosomes from human CD34+ stem cells mediate their proangiogenic paracrine activity. *Circ Res.* 2011; 109: 724–8.
74. **Senger DR, Davis GE.** Angiogenesis. *Cold Spring Harb Perspect Biol.* 2011; 3: pii: a005090.
75. **Ribatti D, Nico B, Crivellato E.** The role of pericytes in angiogenesis. *Int J Dev Biol.* 2011; 55: 261–8.